Separation Science and Technology
Publication details, including instructions for authors and subscription information:
http://www.informaworld.com/smpp/title~content=t713708471

Treatment of Textile Dye Plant Effluent by Nanofiltration Membrane

Yazhen Xu[a]; Rémi E. Lebrun[a]; Pierre-Jean Gallo[b]; Pierre Blond[b]
[a] UNIVERSITÉ DU QUÉBEC À TROIS-RIVIÈRES, QUÉBEC, CANADA [b] I.C.P.I. LYON, LYON, CEDEX 02, FRANCE

Online publication date: 15 September 1999

To cite this Article Xu, Yazhen , Lebrun, Rémi E. , Gallo, Pierre-Jean and Blond, Pierre(1999) 'Treatment of Textile Dye Plant Effluent by Nanofiltration Membrane', Separation Science and Technology, 34: 13, 2501 — 2519
To link to this Article: DOI: 10.1081/SS-100100787
URL: http://dx.doi.org/10.1081/SS-100100787

SEPARATION SCIENCE AND TECHNOLOGY, **34**(13), pp. 2501–2519, 1999

Treatment of Textile Dye Plant Effluent by Nanofiltration Membrane

YAZHEN XU and RÉMI E. LEBRUN*
DÉPARTEMENT DU GÉNIE CHIMIQUE
ÉCOLE D'INGÉNIERIE
UNIVERSITÉ DU QUÉBEC À TROIS-RIVIÈRES
C.P. 500, TROIS-RIVIÈRES, QUÉBEC G9A 5H7, CANADA

PIERRE-JEAN GALLO and PIERRE BLOND
I.C.P.I. LYON
31, PLACE BELLECOUR
69288 LYON CEDEX 02, FRANCE

ABSTRACT

The study was concerned primarily with characterization of the NF45 membrane. Its pure water permeability, the mass transfer coefficient of NaCl, and the mean radius of the membrane pores were determined. Experiments run with five pure dye solutions and an industrial dye pulp solution confirmed the potential of nanofiltration membrane separation for the treatment of textile dye plant effluent. The effects of such significant parameters as initial solution concentration, transmembrane pressure, and type of dye on two fundamental characteristics of nanofiltration (flux and separation factor) were studied.

Key Words. Nanofiltration; Membrane; Characterization; Treatment; Dye; Effluent

INTRODUCTION

Wastewater from the textile industry is characterized by strong color and a high concentration of organic carbon. In general, the color is not removed by

* To whom correspondence should be addressed. E-mail: Remi_Lebrun@uqtr-uquebec.ca

typical wastewater processing. One general method of reducing color is by ozonation. From the available information, it is evident that ozonation can achieve high color removal, reduce the level of organic compounds, improve biodegradability, destroy phenols, and insure disinfection. One of drawbacks of ozonation is cost (1). Moreover, even high doses of ozone do not completely convert the organics to carbon dioxide and water, particularly for dye wastes containing surfactants and suspended matter (2).

Membrane techniques, characterized by their ability to clarify, concentrate, and continuously separate, are potentially interesting for effluent treatment through recycling. In the last few years, the treatment of industrial waste effluents by membrane processes has gained more and more interest because of technical, economical, and political reasons. Technically, the basic technology of process engineering has been developed; Economically, the shortage of water and the increasing cost of auxiliary chemicals and energy have pushed this technology; Politically, the increasing interest of government and people to environmental problems has forced industries to observe severe environmentally safe procedures (3).

The performance of microfiltration depends on the composition of the waste, which can be improved by the addition of ionic micelles (4). Ultrafiltration (UF) can remove some of the dyes from a waste feed solution, the separation depends on the solution proprieties and the UF unit operating parameters (5). Membrane filtration coupled with ozonation of the retentate was used for the treatment of colored textile wastewater. A selected membrane filtration process generates a permeate with over 99% of the color and copper removed, while 85% of salts by mass and 85% of the original water were reusable (6). Nanofiltration, a membrane process located between ultrafiltration and reverse osmosis, combines the advantages of ultrafiltration by using moderate pressure and those of reverse osmosis by separating solutions, makes it possible to recover 97–99% of the water from some effluent stream, with sufficient quality to recycle the permeate into the dyeing process. The aim of introducing membrane filtration is not only to reduce the water and wastewater streams, but also to minimize the consumption of dyeing process chemicals and to save energy. Many effluent streams are hot, and they are currently led to drain. Recycling such streams will reduce the energy consumed by using them to heat fresh water (7).

This study was concerned primarily with characterization of the NF45 membrane. We investigated the potential of a nanofiltration membrane for the treatment of textile dye plant effluent by experiments run with five pure dye solutions and an industrial dye pulp solution. The effects of such significant parameters as initial solution concentration, transmembrane pressure, and type of dye on two fundamental characteristics of nanofiltration (flux and separation factor) were also studied.

MATERIAL AND METHODS

The NF45 membrane, manufactured by Filmtec, was selected from a choice of three types of nanofiltration membranes. It is a hydrophilic membrane with pore diameters between 2 and 5 nm. It displays an isoelectric point of 6.5 (8) and hence is electrically positive for pH values lower than 6.5 and negative for pH values greater than 6.5.

The experimental apparatus is a simple closed circuit. The system schema, shown in Fig. 1, comprises three essential sections:

- Supply: Prior to entering the filtration modules, the solution is prefiltered by a 5-μm filter. It is circulated via a diaphragm pump equipped with a pulse shock absorber.
- Nanofiltration: Four flat nanofiltration modules have been installed in series, each module having a membrane surface of 14.2×10^{-4} m^2.
- Measurement: The permeate flow from each module is determined by weight. The concentration of the circulation solution and the permeate are determined either by a conductometer for the NaCl solution or by a visible UV spectrophotometer for the dye solutions. In all cases, the parameter (conductivity or transmittance factor) is calibrated according to the concentration beforehand.

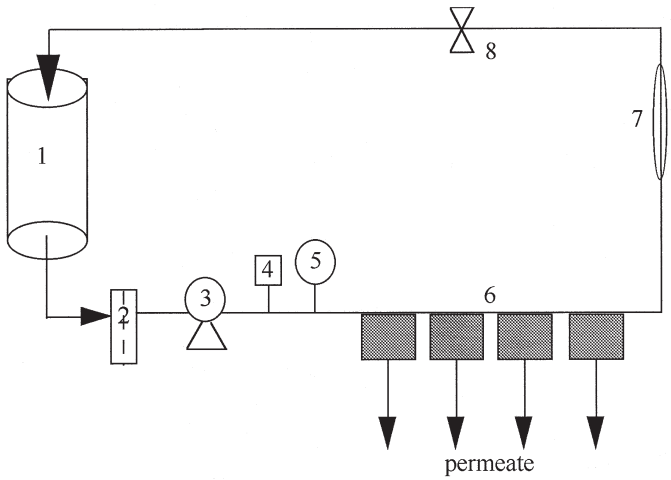

1- Pyrex 101 Vessel 2- Pre-filter, 5 μm 3-Diaphragm Pump

4- Thermocouple and analog thermometer 5- Pressure Gauge

6- Filtration modules in series 7- Flow meter 8- Valve

FIG. 1 Schematic representation of the experimental nanofiltration apparatus.

MARCEL DEKKER, INC.
270 Madison Avenue, New York, New York 10016

Experimental studies were run in two stages: a membrane characterization phase and a nanofiltration phase for dye effluent treatment.

Membrane Characterization

This phase involved measurement of membrane permeability, determination of mass transfer coefficient, and evaluation of membrane pore size.

The nanofiltration process is characterized by both the permeate flow and the separation factor. The global separation factor and the intrinsic separation factor are defined respectively by the following expressions:

Global separation factor

$$f = (C_b - C_p)/C_b = 1 - C_p/C_b \quad (1)$$

Intrinsic separation factor

$$f' = (C_w - C_p)/C_w = 1 - C_p/C_w \quad (2)$$

where C_b, C_w, and C_p are the molar concentration of feed solution, concentrated boundary solution, and permeate solution, respectively (mol/m^3).

Measurement of Permeability

Tests were run using pure water under varying pressures to measure membrane permeability. The system was operated with demineralized water at a pressure 20% greater than the maximum operating pressure for 1 hour in order to compact the membrane. Membrane permeability is determined by

$$A_i = J\mu/\Delta P \quad (3)$$

where A_i = pure water permeability of membrane (m)
J = permeate flux (m/s)
ΔP = transmembrane pressure (Pa)
μ = viscosity of water (Pa·s)

Determination of Mass Transfer Coefficient

Experiments were run using salt water to measure the mass transfer coefficient of NaCl. A saline solution was introduced into the system. After each experiment, the system was flushed with a solution of 2% Ultrasil 10, followed by flushing with demineralized water.

Taking into account the diffusive retroflux due to osmotic pressure from the concentration difference on either side of the membrane, and by ignoring the resistance of the boundary layer, Eq. (3) is modified as follows (9):

$$J = A_i\,[\Delta P - \pi(C_w) + \pi(C_p)]/\mu \quad (4)$$

MARCEL DEKKER, INC.
270 Madison Avenue, New York, New York 10016

Therefore:

$$\pi(C_w) = \Delta P - \mu J/A_i + \pi(C_p) \tag{5}$$

On the other hand, the osmotic pressure for a dilute ionized solution can be calculated according to van't Hoff's equation:

$$\pi(C) = \Sigma_i RTC \tag{6}$$

where $\pi(C)$ = osmotic pressure of a solution with molar concentration C (Pa)
R = perfect gas constant, $R = 8.314$ (J/mol/K)
T = absolute temperature (K)
Σ_1 = number of ions per molecule of solute, $\Sigma_i = 2$ for NaCl

Hence the molar concentration of concentrated boundary solution C_w can be calculated by

$$C_w = \frac{\Delta P - \mu J/A_i}{\Sigma_i RT} + C_p \tag{7}$$

Moreover, by running a mass balance in the boundary layer (film model), a formula for the calculation of the permeate flux can be obtained as follows:

$$J = k \ln\left(\frac{C_w - C_p}{C_b - C_p}\right) \tag{8}$$

Therefore:

$$k = J/\ln\left(\frac{C_w - C_p}{C_b - C_p}\right) \tag{9}$$

where k is the mass transfer coefficient on the high pressure side of the membrane (m/s).

According to Robinson and Stokes (10), if the viscosity of the solution approaches that of pure water, the value of the mass transfer coefficient for a solution can be calculated from that for a sodium chloride solution by the following formula:

$$k_{solute} = k_{NaCl}\left(\frac{(D_{AB})_{solute}}{(D_{AB})_{NaCl}}\right)^{2/3} \tag{10}$$

where D_{AB} is the diffusivity of solute A in solvent B (m^2/s).

Evaluation of Membrane Pore Size

The methods for determining the diameters of active pores which are directly involved in membrane separation are generally classified in two groups:

- Direct methods of membrane observations such as electron microscopy, x-rays, etc.
- Indirect methods involving the use of one or more fluids, determining membrane characteristics as a function of membrane behavior vis-à-vis these fluids, such as the permeation speed, the retention rate, etc.

This study employed an indirect method based on the surface force–pore flow model (SFPF) which was developed for ultrafiltration and reverse osmosis transport by Sourirajan and Matsuura (11). Lebrun et al. (12) used this model to examine the membrane process. In this model, the pores on the membrane surface are assumed equivalent to circular cylindrical pores, with or without pore size distribution; and the solute–membrane material interactions relative to solvent (water) are expressed in terms of the electrostatic surface potential function. The transport of solute and solvent through the membrane pores is governed by such surface forces, together with frictional forces and solution velocity profiles within the pores. The intrinsic separation factor is expressed by the following dimensionless expression:

$$f' = 1 - \frac{1}{\int_0^1 \alpha(\rho)\rho d\rho} \int_0^1 \frac{e^{\alpha(\rho)}}{1 + \dfrac{b(\rho)}{e^{-\phi(\rho)}}\left(e^{\alpha(\rho)} - 1\right)} \alpha(\rho)\rho d\rho \qquad (11)$$

where ρ = radial dimensionless distance, $\rho = r/R_a$
r = radial distance (m)
R_a = effective radius of membrane pores available for fluid flow, $R_a = R_b - D_w$ (m)
R_b = radius of membrane pores (m)
D_w = water molecule radius, $D_w = 0.87 \times 10^{-10}$ m
$\alpha(\rho)$ = dimensionless solution velocity profile in the pore:

$$\alpha(\rho) = \frac{\Delta P R_a^2}{4 D_{AB} \mu}\left(1 - \rho^2\right) \qquad (12)$$

$b(\rho)$ = frictional force function:

$$b(\rho) = \begin{cases} 44.57 - 416.2\lambda + 934.9\lambda^2 + 302.4\lambda^3, & \text{if } 0.22 < \lambda < 1 \\ (1 - 2.104\lambda + 2.09\lambda^3 - 0.95\lambda^5)^{-1}, & \text{if } \lambda \le 0.22 \end{cases} \qquad (13)$$

λ = steric hindrance of the solute at the interface, $\lambda = d/R_b$
d = steric hindrance parameter of the solute at the interface (m). For a given solute, this is dependent on the chemical nature of

MARCEL DEKKER, INC.
270 Madison Avenue, New York, New York 10016

the solvent and the material of the membrane surface; the value of the Stokes' radius can be used as an approximation

$\phi(\rho)$ = dimensionless potential surface function:

$$\phi(\rho) = \begin{cases} \infty, & \text{when } \left(\dfrac{R_b}{R_a} - \rho\right) \le \dfrac{d}{R_a} \\ \dfrac{A}{R_b - \rho R_a} - \dfrac{B}{(R_b - \rho R_a)^3}, & \text{when } \left(\dfrac{R_b}{R_a} - \rho\right) > \dfrac{d}{R_a} \end{cases} \quad (14)$$

A = electrostatic repulsive force constant (m)
B = attractive or repulsive force constant (m^3)

On the one hand, Eq. (11) shows that for a given solution and fixed operating conditions, the intrinsic separation factor depends only on the membrane pore radius. On the other hand, the intrinsic separation factor can be calculated from C_w and C_p by Eq. (2). Hence Eq. (11) can be numerically resolved to determine the mean membrane pore radius.

The study by Sourirajan and Matsuura (11) helped clarify the parameters characterizing some azo dyes in solution, as well as those referring to a wide range of membranes. In the present study, experiments were performed using Orange II dye. The parameters for characterizing Orange II are shown in Table 1.

Nanofiltration Experiments on the Treatment of Dying Effluent

Five solutions of pure dye and one of reactive dye pulp were selected for our study. The reactive dye pulp (from an industrial effluent) is considered to be representative of an actual effluent, and the amount of dye in the mixture is unknown. The circulation flow rate is around $2 \times 10^{-5} m^3/s$ and the operating temperature is around 25°C. The principal characteristics of these dyes are shown in Table 2. The same protocol used in previous studies was followed.

TABLE 1
Parameters for Characterizing Orange II (11)

Diffusivity D_{AB} (m^2/s)	5.28×10^{-10}
Stokes' radius d (m)	6.56×10^{-10}
A (m)	3.4×10^{-10}
B (m^3)	987.5×10^{-30}

TABLE 2
Principal Characteristics of Five Pure Dyes and a Reactive Dye Pulp

	Dyes					
	Orange II	Safranine-o-	Eosine B	Fast Blue	Fast Green	Pulp
Molar mass (g/mol)	350.0	350.0	624.1	475.5	808.9	637.4
Solvent	Water	Water	Water	Water	Water	Water + urea
Solubility (kg/m^3)	130	—	50	70	60	—

RESULTS AND DISCUSSION

Water Permeability

Experimental results (Fig. 2) show that the pure water permeability of the membrane decreases markedly with pressure even though the membrane is compressed beforehand for 1 hour by a pressure 20% greater than the maximum operating pressure. The decrease in membrane permeability is probably due to incomplete membrane compaction, which would suggest that either a higher compaction pressure or a longer compaction time should be used.

Mass Transfer Coefficient of NaCl

Experiments with NaCl were run at different pressures. Figure 3 shows that for pressures below 10^6 Pa, the phenomenon of concentration polarization is

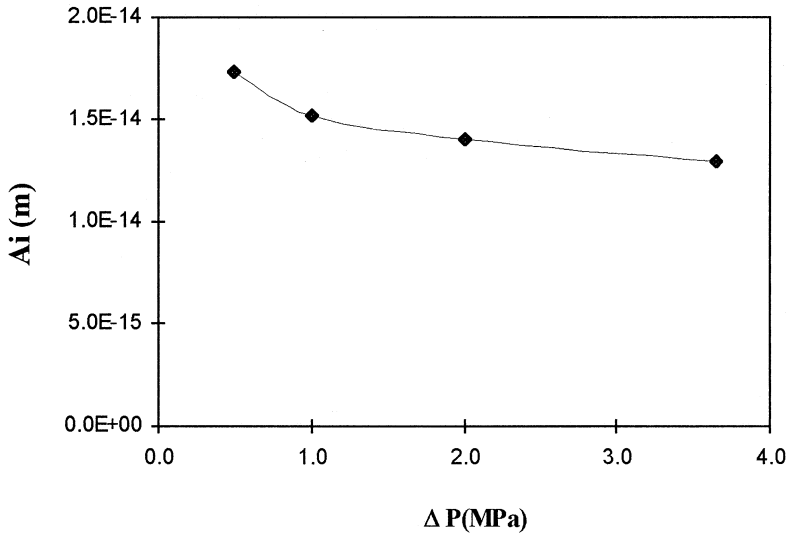

FIG. 2 Evolution of pure water membrane permeability versus transmembrane pressure.

MARCEL DEKKER, INC.
270 Madison Avenue, New York, New York 10016

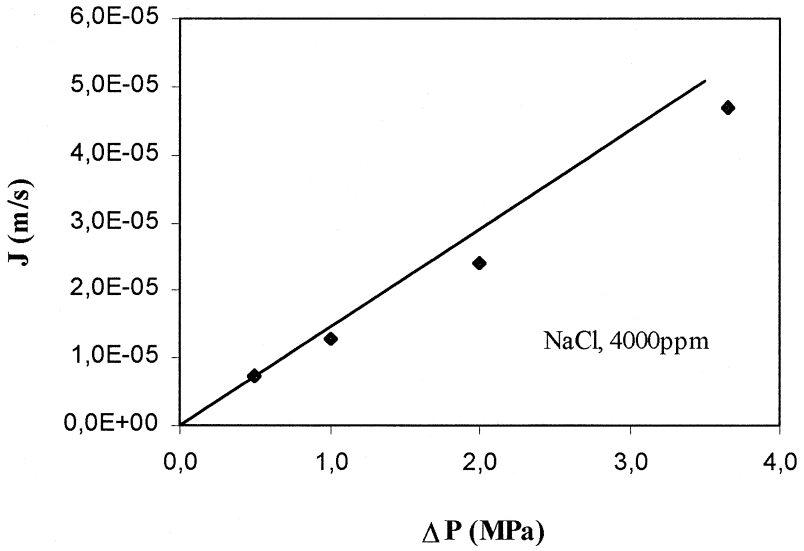

FIG. 3 Evolution of permeate flux versus transmembrane pressure for NaCl.

not significant. The feed concentration C_b is very close to the wall concentration C_w, so Eq. (9) is not appropriate for calculating the value of the mass transfer coefficient. For pressures above 10^6 Pa, a mean value of $k_{NaCl} = 5.8 \times 10^{-5}$ m/s was obtained.

Mean Membrane Pore Radius

The nanofiltration of Orange II dye solution was run under different pressures. The mass transfer coefficient of Orange II, $k_{\text{orange II}}$, can be calculated from Eq. (10). Since the value of k_{NaCl} is a mean value for $P > 10^6$ Pa, the obtained value of $k_{\text{orange II}}$ is also for $P > 10^6$ Pa.

$$k_{\text{orange II}} = k_{NaCl}\left(\frac{(D_{AB})_{\text{orange II}}}{(D_{AB})_{NaCl}}\right)^{2/3}$$

$$= 5.8 \times 10^{-5}\left(\frac{0.528 \times 10^{-9}}{1.61 \times 10^{-9}}\right)^{2/3}$$

$$= 2.76 \times 10^{-5}\ \text{m/s}$$

For Orange II dye solution, the molar concentration of the concentrated boundary solution can not be calculated by Eq. (7) due to some unknown properties of the dye solution. However, once the mass transfer coefficient of Orange II, $k_{\text{orange II}}$, has been calculated, the molar concentration of the concentrated boundary solution can be deduced from Eq. (9):

$$C_w = C_p + (C_b - C_p)\exp(J/k_{\text{orange II}}) \qquad (15)$$

MARCEL DEKKER, INC.
270 Madison Avenue, New York, New York 10016

The concentration polarization rate is defined as the ratio C_w/C_b. The calculated results show that the concentration polarization rate becomes more significant as the pressure rises and as the experiment proceeds. Figures 4a-b display the evolution of C_w/C_b as a function of pressure and of time, respectively, during the same experiment.

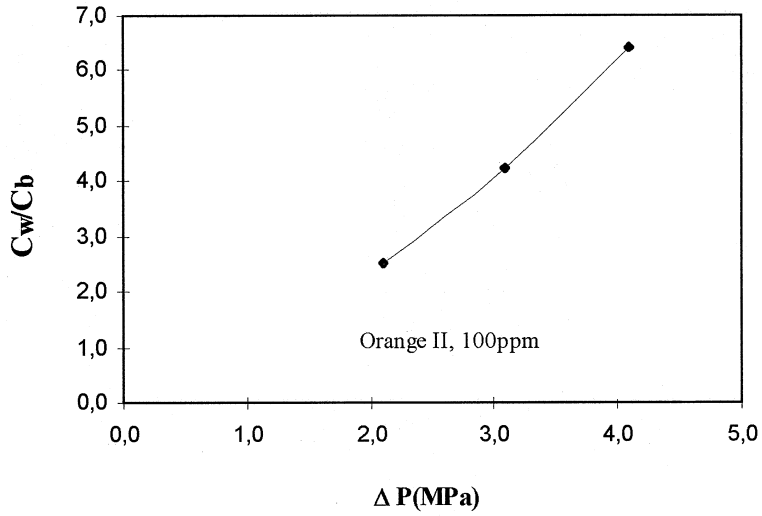

(a)

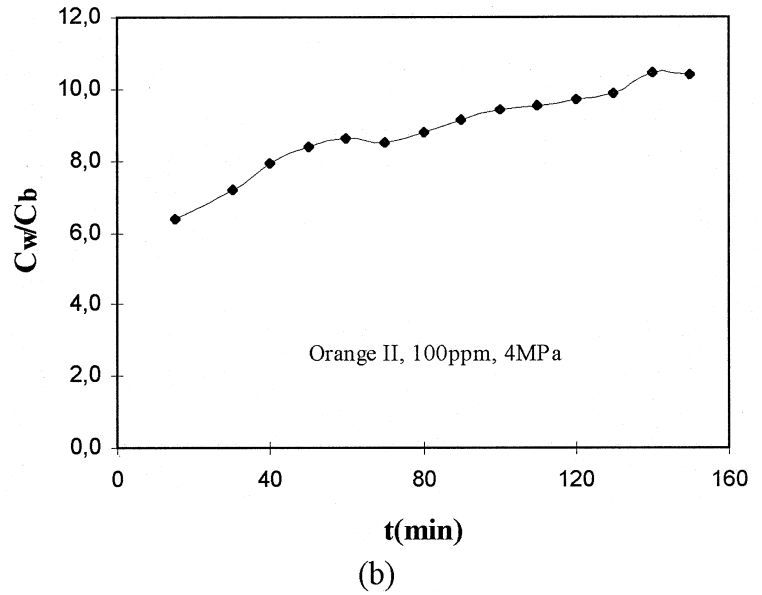

(b)

FIG. 4 Evolution of C_w/C_b as a function of pressure or as a function of time.

MARCEL DEKKER, INC.
270 Madison Avenue, New York, New York 10016

TABLE 3
Experimental and Calculated Values of the Intrinsic Separation Factor

	ΔP (MPa)		
	2.0	3.0	4.0
Experimental f' (%)	99.64	99.86	99.85
Calculated f' (%)	99.71	99.79	99.82

The mean pore radius of the NF45 membrane, 0.76 nm, was obtained by resolving Eq. (11). The intrinsic separation factors have been recalculated from the mean pore radius at each pressure level; the results are shown in Table 3.

Application in Dye Effluent Treatment

Figures 5a-b depict the evolution of the four parameters over time during the nanofiltration of Safranine-o- dye at an initial concentration of 145 ppm. The permeate flux was observed to remain practically constant over time. The global separation factor increased with time at the beginning and stabilized rapidly at around 99.5%. The permeate concentration decreased over time at the beginning and stabilized at approximately 0.7 ppm, while the circulation concentration rose gradually over time.

Influence of the Initial Concentration

In nanofiltration membrane separation, concentration certainly plays a significant role. In general, the higher the concentration, the higher is the osmotic pressure, and, consequently, the permeate flux is lower. For Orange II solution, Figs. 6a-b show that the permeate flux is always higher at lower solution concentration. However, the global separation factor is higher at lower solution concentration only after 60 minutes of operation. On the other hand, for Safranine-o- solution, Figs. 6c-d show that the permeate flux and the global separation factor are all higher as the concentration is higher. The phenomenon can be explained by the significance of the interaction forces. Unfortunately, the experimental results can not be fully explained due to insufficient information on the solution charge.

Influence of Transmembrane Pressure

The influence of transmembrane pressure on permeate flux and on global separation factor was evaluated for different dyes at a concentration close to 500 ppm. Figures 7a-b show that the effect of pressure on the permeate flux and on the global separation factor differed, depending on the dye. For Fast

MARCEL DEKKER, INC.
270 Madison Avenue, New York, New York 10016

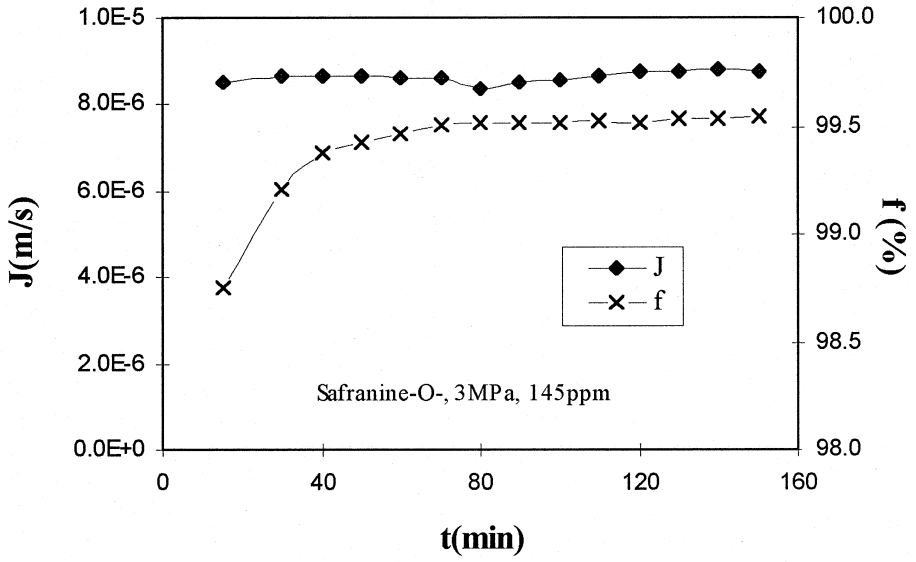

(a)

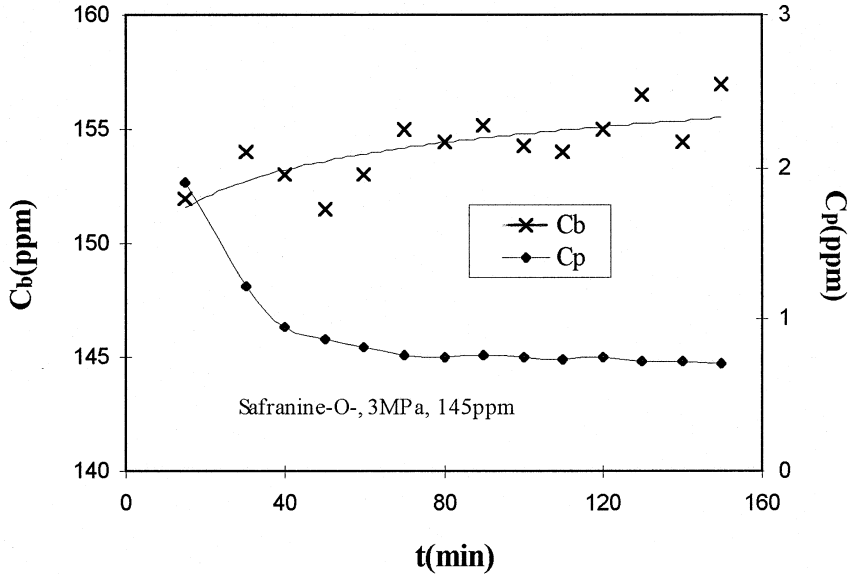

(b)

FIG. 5 Evolution of four parameters as a function of time for Safranine-o- solution.

Green solution, the permeate flux increased in a linear mode with pressure; the separation factor reached 99.9% and remained constant. This signifies that mass transfer is not a limiting factor as regards operating pressure and the phenomenon of concentration polarization is of little importance. For Orange II

MARCEL DEKKER, INC.
270 Madison Avenue, New York, New York 10016

and Eosine B solutions, the permeate flux rose more rapidly with pressure at the beginning and increased more slowly at high pressure. This indicates that concentration polarization begins to intervene in the range of operating pressure. For Fast Blue solution, the permeate flux fell slightly with pressure at the

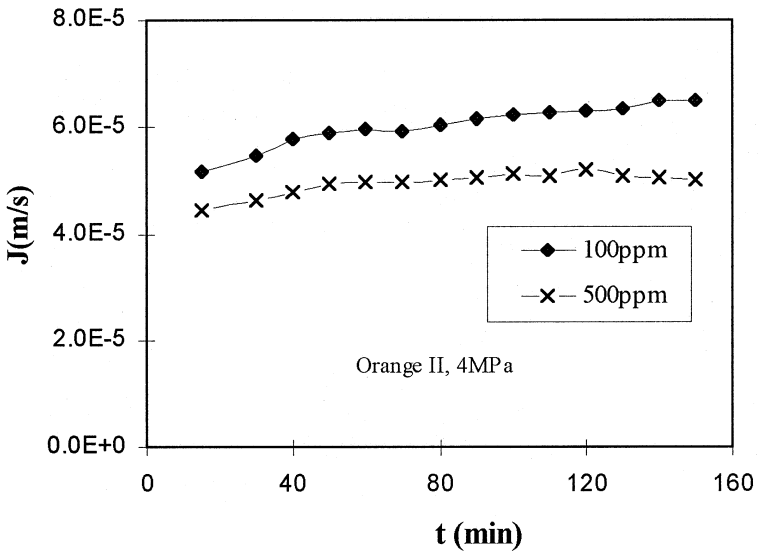

(a)

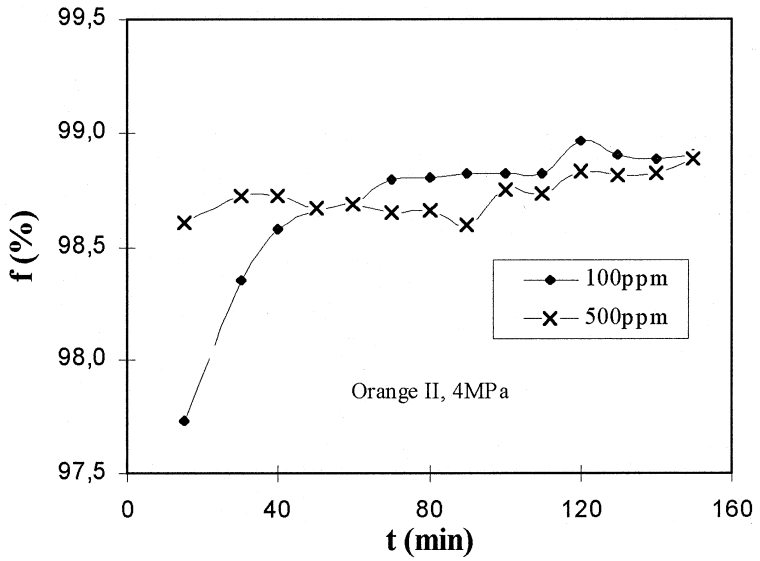

(b)

FIG. 6 Influence of concentration on the permeate flux and on the global separation factor.

(continued)

MARCEL DEKKER, INC.
270 Madison Avenue, New York, NY 10016

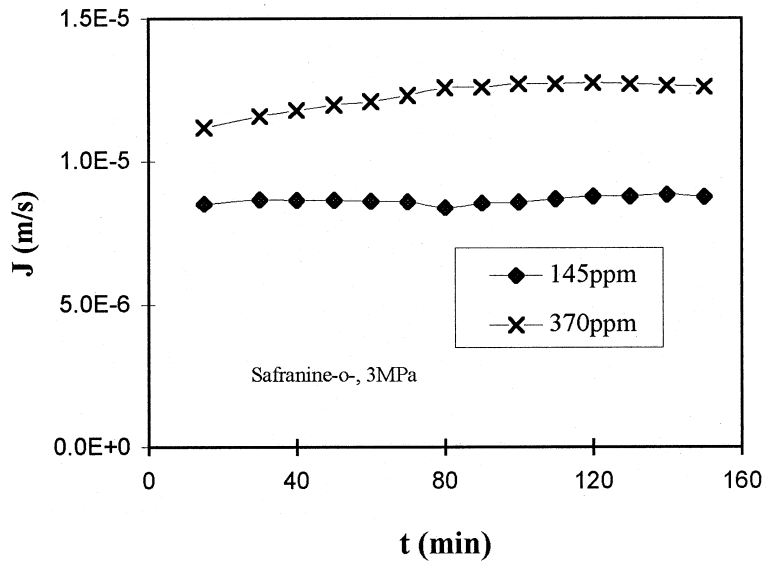

(c)

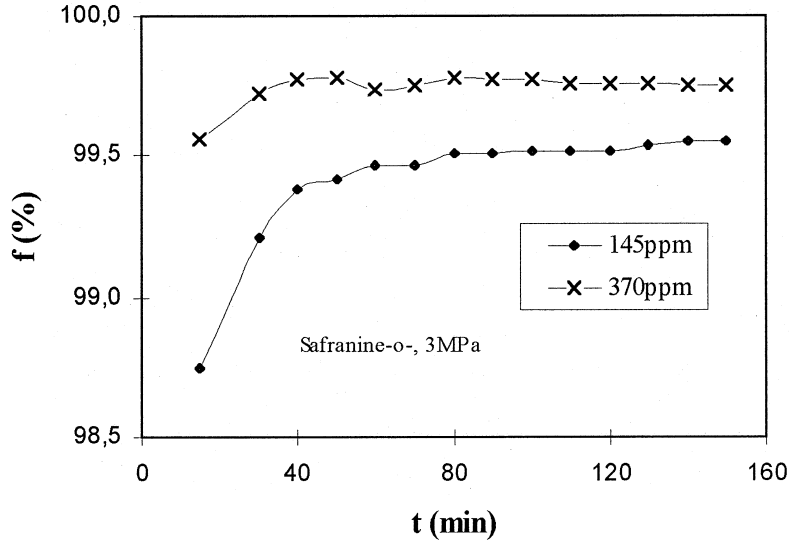

(d)

FIG. 6 Continued.

beginning and dropped further with high pressure, which indicates that the concentration polarization is significant in this case.

The influence of transmembrane pressure on permeate flux and on global separation factor was also evaluated for the reactive dye pulp of 1000 ppm.

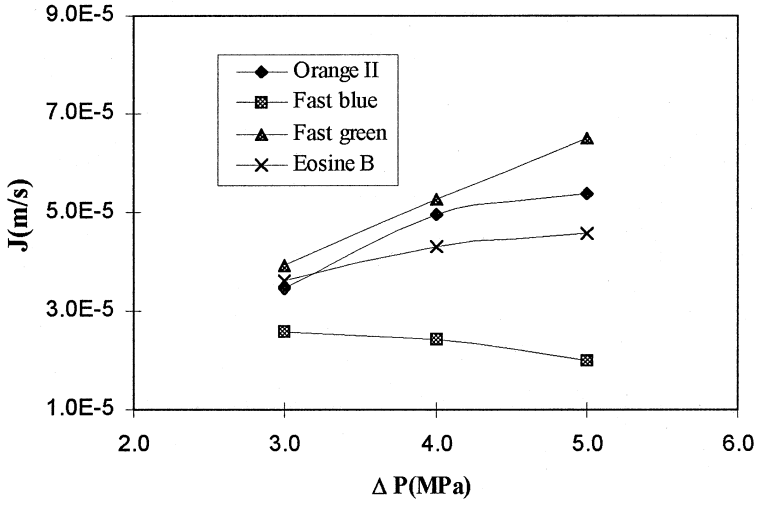

(a)

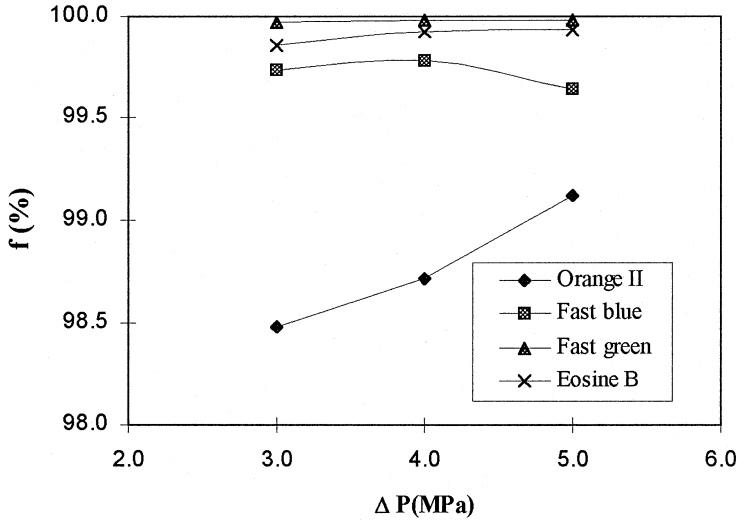

(b)

FIG. 7 Influence of pressure on the permeate flux and on the global separation factor for different dyes.

Figure 8a shows that the permeate flux is greater when the pressure is higher in the beginning; however, the permeate flux under higher pressure drops markedly after a certain period of operation. It appears that concentration polarization is affecting the filtration of the reactive dye pulp at this pressure

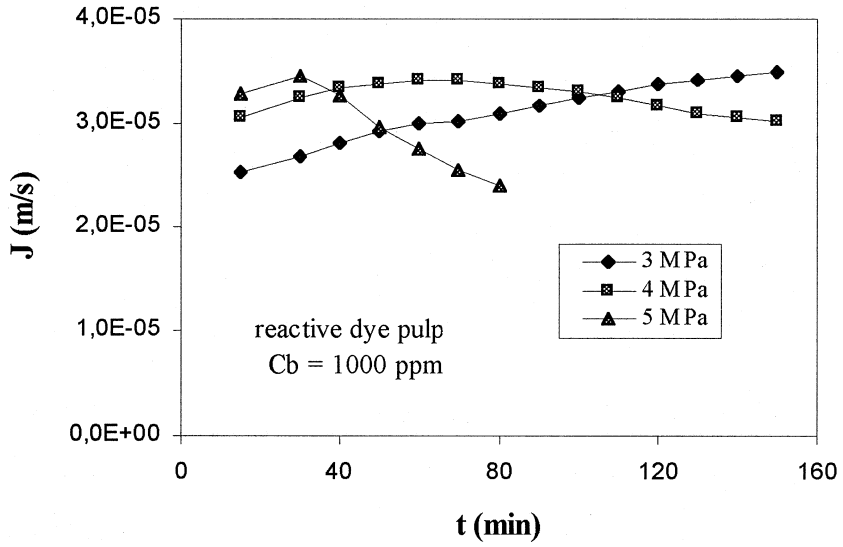

(a)

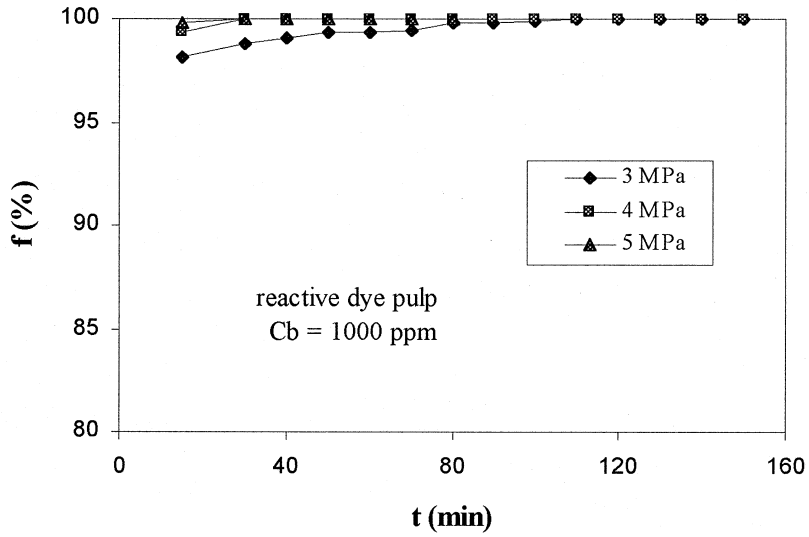

(b)

FIG. 8 Evolution of permeate flux and global separation factor versus time for reactive dye pulp.

level. Figure 8b shows that the global separation factor reaches 98% in the beginning and rapidly rises to 100% for all testing pressures. The difference between permeate flux and global separation factor behaviors can be explained by the existence of concentration polarization at higher pressure.

Influence of Dye Types

The behavior of some dyes with similar molar masses was compared. Orange II and Safranine-o- have a molar mass of 350 g/mol (Table 2). Figures 6a-d show that the effect of initial concentration on the flux and the separation factor differs for these two dyes which have similar molar masses.

CONCLUSION

Characterization of the NF45 membrane showed that, even though the membrane was compressed beforehand by a pressure 20% greater than the maximum operating pressure for 1 hour, pure water permeability decreases with increasing transmembrane pressure, which suggests that either a higher compaction pressure or a longer compaction time should be used. On the other hand, it showed that the film model is not appropriate for calculating the mass transfer coefficient when the pressure is low because of the nonexistence of concentration polarization.

Experiments run with five pure dye solutions and an industrial dye pulp solution confirmed the potential of nanofiltration membrane separation for the treatment of textile dye plant effluent. The global separation factor is greater than 98.5% within the range of dyes studied. The study on the effects of such significant parameters as initial solution concentration, transmembrane pressure, and type of dye on two fundamental characteristics of nanofiltration showed that the identification of transfer phenomena in dye solutions during nanofiltration is complex. The definition of the dominant transfer mechanisms in nanofiltration is based not only on experimentation but also on knowledge of the properties of the solution undergoing treatment and those of the membrane.

NOMENCLATURE

A	electrostatic repulsive force constant (m)
A_i	pure water permeability of membrane (m)
B	attractive or repulsive electrostatic force constant (m^3)
$b(\rho)$	frictional force function
C	molar concentration of solution (mol/m^3)
C_b	feed concentration (mol/m^3)
C_p	permeate concentration (mol/m^3)
C_w	wall concentration (mol/m^3)
d	steric hindrance parameter of the solute at the interface (m)
D_{AB}	diffusivity of solute A in solvent B (m^2/s)
D_w	radius of a water molecule
f, f'	global separation factor and intrinsic separation factor, respectively
J	permeate flux (m/s)

MARCEL DEKKER, INC.
270 Madison Avenue, New York, New York 10016

k	mass transfer coefficient (m/s)
P	pressure (Pa)
r	radial distance (m)
R	perfect gas constant (J/mol/K)
R_a	effective radius of membrane pores available for fluid flow (m)
R_b	membrane pore radius (m)
T	absolute temperature (K)

Greek Letters

$\alpha(\rho)$	dimensionless solution velocity profile in the pore
Δ	gradient
$\phi(\rho)$	dimensionless potential surface function
ρ	radial dimensionless distance
λ	steric hindrance parameter of the solute at the interface
μ	fluid viscosity (Pa·s)
Σ_i	number of ions per molecule of solute
π	osmotic pressure (Pa)

ACKNOWLEDGMENTS

We thank Hydro-Québec for its financial support which funded the publication of these results. Our thanks also go to Électricité de France for its support during the study of the city of Lyon and for having awarded Le Prix Innovalyon to Pierre-Jean Gallo, and furthermore to Hayka Inc. for the gracious loan of its rigs.

REFERENCES

1. F. Gahr, F. Hermanutz, and W. Oppermann, "Ozonation—An Important Technique to Comply with New German Law for Textile Wastewater Treatment," *Water Sci. Technol.*, *30*, 255–263 (1994).
2. S. H. Lin and W. Liu, "Treatment of Textile Wastewater by Ozonation in a Packed-Bed Reactor," *Environ. Technol.*, *15*, 299–311 (1994).
3. S. N. Gaeta and U. Fedele, "Recovery of Water and Auxiliary Chemicals from Effluents of Textile Dye Houses," *Desalination*, *83*, 183–194 (1991).
4. M. T. Pessoa de Amorim, "Membrane Filtration Techniques in the Recovery of Dyes, Chemicals and Treatment of Textile Wastewater," *Environ. Pollut. 1-ICEP*. *1*, 686–691 (1991).
5. J. Watters, E. Biagtan, and O. Senler, "Ultrafiltration of a Textile Plant Effluent," *Sep. Sci. Technol*. *26*(10&11), 1295–1313 (1991).
6. J. Wu, M. A. Eiteman, and S. E. Law, "Evaluation of Membrane Filtration and Ozonation Processes for Treatment of Reactive-Dye Wastewater," *J. Environ. Eng*. pp. 272–277 (March 1998).
7. C. E. Nielson, "Recycling of Wastewaters from Textile Dyeing Using Crossflow Membrane Filtration," *Ibid*., pp. 593–595 (September/October 1994).

8. T. Courtois, *Caractérisation des membranes de nanofiltration*, Presented at 1er Atelier "Nanofiltration et Application" France-Canada, Trois-Rivières, Quebec, Canada, June 2–4, 1997.
9. R. A. Robinson and R. H. Stokes, *Electrolyte Solutions*, 2nd ed., Butterworths, London, 1959.
10. M. C. Porter, "Membrane Filtration," in *Handbook of Separation Techniques for Chemical Engineers* (Schweitzer, Ed.), McGraw-Hill, New York, NY, 1979.
11. S. Sourirajan and T. Matsuura, *Reverse Osmosis/Ultrafiltration Principles*, Division of Chemistry, National Research Council Canada, Ottawa, Canada, 1985.
12. R. E. Lebrun, C. R. Bouchard, A. L. Rollin, T. Matsuura, and S. Sourirajan, "Computer Simulation of Membrane Separation Processes," *Chem. Eng. Sci.*, *44*(2), 313–320 (1989).

Received by editor May 26, 1998
Revision received February 1999

Request Permission or Order Reprints Instantly!